

VIBRATIONAL SPECTRA OF TRANSITION METAL HEXAFLUORIDE CRYSTALS. I. ORTHORHOMBIC MoF_6 , WF_6 , AND UF_6 NEAT CRYSTALS*

E.R. BERNSTEIN and G.R. MEREDITH**

*Department of Chemistry, Colorado State University,
Fort Collins, Colorado 80523, USA*

Received 11 March 1977

Neat crystal Raman spectra of orthorhombic MoF_6 , WF_6 , and UF_6 are presented and discussed. This work lays the foundation for presentation of two-particle and total band structures in the two following papers. The neat crystal spectra are interpreted in terms of an internal-external mode separation and a conventional factor group analysis. In general, these data lead to four essential conclusions concerning hexafluoride crystals: (a) Fermi resonance plays an important role in producing the observed energy and intensity differences in this series; (b) $k = 0$ exciton structures are remarkably similar in the three crystals; (c) similarities and differences between these solids can be directly correlated with molecular parameters such as dipole derivatives, polarizabilities, etc.; and (d) phonons (external modes) can be neatly separated into rotational and translational normal modes.

1. Introduction

The vibrational properties of the series of hexafluoride molecules have been extensively studied both theoretically and experimentally [1]. The octahedral structure makes this series a textbook example of vibrational analysis (for those compounds not subject to Jahn-Teller instability). With the development of narrow line tunable diode lasers, even the disadvantage of the relatively high molecular moment of inertia (closely spaced rotational structure) has to a large extent been overcome [2]. With the use of noble gas ion lasers in Raman spectroscopy more and finer details of the spectra have been observed [3–6]. Coupled with these experimental advances the determination of accurate potential functions containing various interactions has progressed markedly [4–7].

Aside from the interest in the molecular properties, there have been few studies of the vibrational characteristics of these systems in condensed phases. Perhaps the sparsity of solid state investigations has been due to the experimental difficulties inherent in

these systems. Of the studies in the literature, one made no attempt to understand the details of the solid, even to the point of discussing the factor group [8], another explained large splittings of the UF_6 crystal vibrational spectra solely in terms of site effects [9], and a third attempted to analyze vibrational relaxation rates in the solid from lineshapes ignoring the excitonic contributions to the structure [10].

During the investigation of electronic transitions of ReF_6 [11] in various MF_6 ($M = \text{Re}, \text{Mo}, \text{W}, \text{U}$) crystals, it became apparent that vibrational levels of these molecules evidence substantial exciton couplings. Additionally, two-particle transitions were observed in the ReF_6 vibronic structure. These transitions have also been observed in IrF_6 spectra [12]. To begin to understand the nature of the crystal interactions we have initiated a study of the purely vibrational properties of the closed shell transition metal hexafluoride crystals. Besides corroborating the details of the two-particle transitions we hope to determine parameters of the exciton bands and make comments about the nature of the intermolecular potentials.

In order to keep any one part of this discussion of the crystal vibrational spectra of transition metal hexafluorides from becoming too cumbersome, we have chosen to divide the presentation into three separate

* Supported in part by ARO-D and ONR.

** Present address: Department of Chemistry, University of Pennsylvania, Philadelphia, PA 19174, USA.

papers. In this paper the low temperature neat crystal Raman spectra of UF_6 , WF_6 and MoF_6 will be presented and discussed in terms of simple factor group analyses. The starting point for this analysis employs the octahedral normal modes of the molecules as a basis. Neat crystal phonon spectra have also been observed and characterized for these systems. In the following two papers we will discuss exciton density of states functions (from two-particle and mixed crystal spectra) and total band structures for Mo, W, and UF_6 crystals.

2. Theoretical

The description of the normal modes of an octahedral MF_6 molecule is almost completely determined by symmetry. The six modes consist of three stretching and three bending modes ordered as ν_1 through ν_6 and belonging (in order) to the irreducible representations a_{1g} , e_g , $2t_{1u}$, t_{2g} , and t_{2u} . The exact description of ν_3 and ν_4 depends on the details of the potential functions which determine the amount of mixing of the pure stretching and bending modes. For UF_6 the separation is nearly complete [13]. The simple symmetry predictions are that ν_1 , ν_3 , and ν_5 will be active in Raman scattering, ν_3 and ν_4 will be active in infrared absorption and ν_6 will be inactive.

The low temperature crystal structure of the hexafluorides belongs to the space group Pnma (D_{2h}^{16}). There are four molecules per unit cell at sites of C_s symmetry. The molecular geometry of UF_6 is approx-

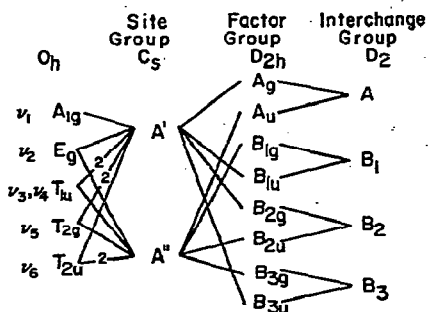


Fig. 1. Correlation diagrams appropriate to the vibrational factor group analysis of transition metal hexafluorides. The two's in the correlation from O_h to C_s irreducible representations indicate that the lower symmetry representation occurs twice.

imately D_{4h} [11], but MoF_6 and WF_6 seem to be closer to O_h symmetry.

By reducing the molecular symmetry to that of the appropriate C_s (site) subgroup of O_h , correlating the irreducible representations of these groups, and correlating the irreducible representations of the site and factor groups (fig. 1), one may obtain the factor group description of the four $k = 0$ crystal functions induced by one molecular excited state function. Similarly, one may deduce the irreducible representations of the phonons by the analogous subduction and induction starting with the molecular description of translational and rotational vectors. The results are summarized in table 1.

Table 1
Summary of factor group predictions for transition metal hexafluoride orthorhombic structure (Pnma)

Molecular mode	O_h irreducible representations	C_s irreducible representations		D_{2h} (factor group) irreducible representations							
		A'	A''	A_g	B_{1g}	B_{2g}	B_{3g}	A_u	B_{1u}	B_{2u}	B_{3u}
Translation	T_{1u}	2	1	2	1	2	1	1	2	1	2
Rotation	T_{1g}	1	2	1	2	1	2	2	1	2	1
ν_1	A_{1g}	1	0	1	0	1	0	0	1	0	1
ν_2	E_g	1	1	1	1	1	1	1	1	1	1
ν_3	T_{1u}	2	1	2	1	2	1	1	2	1	2
ν_4	T_{1u}	2	1	2	1	2	1	1	2	1	2
ν_5	T_{2g}	2	1	2	1	2	1	1	2	1	2
ν_6	T_{2u}	1	2	1	2	1	2	2	1	2	1

Besides the $k = 0$ selection rule for Raman scattering there is also an inversion parity rule. Only gerade states may be created in the crystal from the gerade ground state. Since every site irreducible representation induces two gerade and two ungerade factor group irreducible representations, $2m k = 0$ transitions are expected in the Raman spectra of these crystals in the energy region of a molecular vibration with degeneracy m . Likewise, treating rotations and translations of the whole molecule, twelve $k = 0$ optical phonon peaks are expected in the Raman spectra.

An interesting consequence of the C_s site symmetry is that all molecular vibrations generate Raman allowed factor group states regardless of the free molecule inversion characteristics of the vibrations. Furthermore, since states of the same symmetry may mix

in the crystal, the optical phonons are theoretically expected to be mixed translational and librational motions even at $k = 0$.

3. Review of the vapor phase Raman spectra

Laser Raman spectra of all of the stable, nonphotosensitive hexafluorides have recently been published [3]. In the normal (non Jahn–Teller) compounds, the spectra are quite simple. An intense polarized high energy peak with two weaker depolarized lower energy peaks are the main features. These were assigned as the ν_1 , ν_2 and ν_5 fundamentals. Also some very weak peaks were assigned as combinations and overtones. The strongest of these is the $2\nu_6$ feature. While

Table 2
Summary of neat MoF₆ crystal Raman spectra at 77 K

Stokes shift (cm ⁻¹)	FWHH (cm ⁻¹)	Assignment	Stokes shift (cm ⁻¹)	FWHH (cm ⁻¹)	Assignment		
30.9		phonons	642.43	0.8	ν_2		
36.4			645.12	1.2			
40.7			645.62	0.8			
59.6			652.45	1.2			
66.6			694.60	1.9	ν_3		
72.7			702.63	2.0			
82.7			718.73				
128			721.64				
140				ν_6	742.19	<0.3	ν_1
247.62			<1.5	ν_4	816.9	40	$\nu_2 + 2\nu_6$
252.34	1.1	927.1	38				
261.87	1.0	967.8			$\nu_2 + \nu_5$		
267.25	20	1061.8	10		$\nu_1 + \nu_5$		
272.08		1289.0	7.3		$2\nu_2$		
275.81		1385.59	14		$\nu_1 + \nu_2$		
278.20	1392.91						
316.02		$\nu_4 + \nu_6$	1482.79	1.2	$2\nu_1$		
319.50	3.1	ν_5					
324.78	2.1						
378.3	36		$3\nu_6$				
395.4		$\nu_5 + \nu_6$					
412.5							
454.3		$2\nu_4$					
498.9	11		$4\nu_6$				
526.3							
548.6							
585.6	32	$\nu_4 + \nu_5$					

one might be tempted to consider this a Fermi resonance effect, the correlation of the $2\nu_6$ distance from ν_5 and the $2\nu_6$ intensities relative to ν_5 are not completely systematic. Differences in details of anharmonicities and second order polarizability tensor terms may be responsible for this lack of correlation.

4. Experimental

The details of the experimental procedures and apparatus are by now well known. Briefly, though, samples were prepared in monel vacuum lines and loaded into small pyrex cells of various shapes which were attached to the monel system. Single crystals were grown from the vapor over periods of many weeks at temperatures below the cubic-orthorhombic solid-solid phase transitions. UF_6 crystals were grown at room temperature as they do not exhibit the transition. Crystals were slowly cooled by lowering them into liquid nitrogen. Samples were then supported in-

side a small pyrex dewar and spectra were obtained.

The Raman spectra were obtained on three different laser Raman spectrometers. Since high resolution and wavelength accuracy became important for the investigations, the final data were obtained on a system utilizing diffraction limited optics and micro-positioning mounts in conjunction with an $f/5.8$ 0.5m double monochromator designed to minimize tracking errors. The monochromator was calibrated throughout the range of Raman scattering with approximately 600 Fe-Ne hollow cathode lines using a correction expression devised to incorporate drive screw cam effects. Raman spectra were obtained in second order of a 1200 g/mm grating using the 5145 Å Ar^+ laser line (1-2 W). The standard deviation for one measurement in the calibration fit was less than 0.1 Å; absolute frequency accuracy to better than 0.2 cm^{-1} can be expected. Reproducibility of sharp peaks was frequently seen to be in hundredths of cm^{-1} . It should be noted, though, that the laser was not run with an etalon and the typical 0.15 cm^{-1} width of Ar^+ laser

Table 3
Summary of neat WF_6 crystal Raman spectra at 77 K

Stokes shift (cm^{-1})	FWHH (cm^{-1})	Assignment	Stokes shift (cm^{-1})	FWHH (cm^{-1})	Assignment	
26.0	}	phonons	669.16	0.5	}	
30.7			672.17	0.4		ν_2
35.5			673.62	0.4		
65.5			675.60	0.4		ν_3
72.4			678.89	0.5		
76.5			692.70	0.6		
84.4			698.48	0.6		
115						772.25
147		ν_6	816.1			
240.11	<3	ν_4	828.3			
249.87	<3					
265.85	<3			1058.2	5.2	$\nu_1 + 2\nu_6$
291.4	22	$2\nu_6$	1094.7	10.5	$\nu_1 + \nu_5$	
320.35	}	ν_5	1342		$2\nu_2$	
323.66			2.6	1385		$2\nu_3$
328.31			3.5			
388		$\nu_4 + \nu_6$	1443		$\nu_1 + \nu_2$	
465		$2\nu_4, \nu_5 + \nu_6$	1542.49	<1.8	$2\nu_1$	
607		$\nu_4 + \nu_5$	1552.72			
650		$2\nu_5$				

lines may be a practical limitation of the total accuracy (and observable linewidths).

5. Results and discussion

Tables 2, 3, and 4 list the observed Raman spectral features of the MoF_6 , WF_6 , and UF_6 (77 K) crystals along with the assignments in terms of the molecular (O_h) vibrations. Representative spectra are displayed in figs. 2 through 8. It should be mentioned that no significant orientation (polarization) effects have been observed. The single minor exception to this generalization is a weak doublet in the ν_3 region of UF_6 . The absence of orientation-dependent spec-

tra, even though the laser output was polarized and single crystals were employed in these studies, is probably associated with beam convergence in a randomly oriented biaxial crystal.

The general features of the spectra can be explained in terms of the internal and external vibrations of the molecular entities constituting the crystals. The internal vibrations with a few exceptions are easily associated with the normal coordinates of the octahedral molecules, modified only slightly by the reduced molecular (site) symmetry. The external vibrations appear to be well separated from the internal motions and have been tentatively assigned in terms of an idealized phonon translation and rotation (libration) separation.

Table 4
Summary of neat UF_6 crystal Raman spectra at 77 K

Stokes shift (cm^{-1})	FWHH (cm^{-1})	Assignment	Stokes shift (cm^{-1})	FWHH (cm^{-1})	Assignment			
28.4	}	phonons	510.80	0.4	}			
34.6			516.89	0.35				
47.0			518.29	0.4				
72.5			534.36	0.5				
77.8			586.39	}				
89.8			590.06					
103.2			608.43					
145.82	1.9	}	610.74	}	ν_3			
149.03	2.4		649.08					
155.27	2.2		663.96			}	ν_1	
163.25	2.8		700.3					
175.33	2.1	}	718.2	}	$\nu_2 + \nu_5$			
185.83	1.4		752.1			ν_1 (ReF_6)?		
191.64	1.2		819.4			$\nu_1 + \nu_6$		
197.18	}	ν_5	870.15	}	$\nu_1 + \nu_5$			
206.73			1.3			877.12		
211.22			1.1			887.37		
215.65			1.6			1035.97	54	$2\nu_2$
226.12			1.8			1181.47	30	$\nu_1 + \nu_2, 2\nu_3$
229.64	}	$2\nu_4, \nu_5 + \nu_6$	1327.96	1.6	$2\nu_1$			
308.4			22	399.6	}	$2\nu_5$		
335.7			}	$2\nu_5$			426.0	
374.8	41	452.3			}	$2\nu_5$		
399.6	}	$2\nu_5$	470.0					
426.0			}	$2\nu_5$			491.8	
452.3					36			
470.0	}	$2\nu_5$						
491.8								

5.1. Internal vibrations

Low resolution survey spectra of the fundamental regions are displayed in fig. 2. In these logarithmic traces the totally symmetric ν_1 peak is typically greater than 10^5 cps while the background is less than 10^2 cps. The identification of groupings of features in terms of molecular vibrations follows from the gas phase spectra. The ν_1 , ν_2 , and ν_5 fundamentals and the $2\nu_6$ peaks are in the same regions as in the published spectra. The weaker ν_3 and ν_4 features observed due to loss of molecular inversion symmetry are centered around the frequencies derived from infrared data. The ν_6 features, visible in these traces only for UF_6 , are observed directly here for the first time. As explained in section 2, only $k=0$ components of the bands derived from the fundamental levels are observed.

The ν_1 feature is in all three cases one apparently symmetric peak with width less than 1 cm^{-1} . It is sometimes limited by the monochromator resolving power and laser linewidth. No indication has been seen of the splitting of the A_g and B_{2g} factor group components. This is in keeping with a general view of excitonic interactions as electrostatic multipolar interactions. The lowest multipole sustained by a neutral octahedral molecule is a hexadecapole. Quite like-

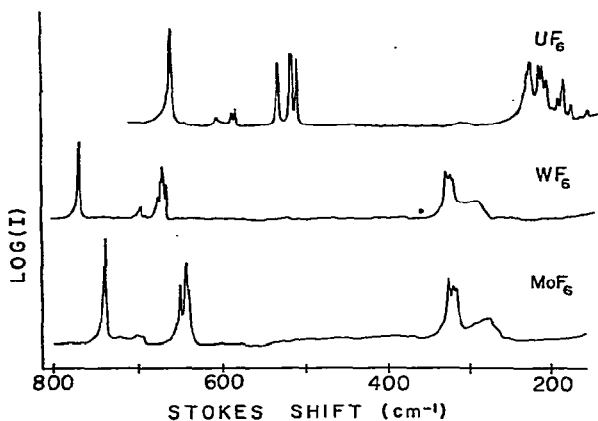


Fig. 2. Low resolution Raman spectra of neat MoF_6 , WF_6 and UF_6 crystals near 77 K. The ordinate is a logarithmic scale. The baselines correspond to less than 100 cps while the ν_1 peaks are approximately 10^5 cps. The assignment of features can be readily seen in tables 2, 3 and 4.

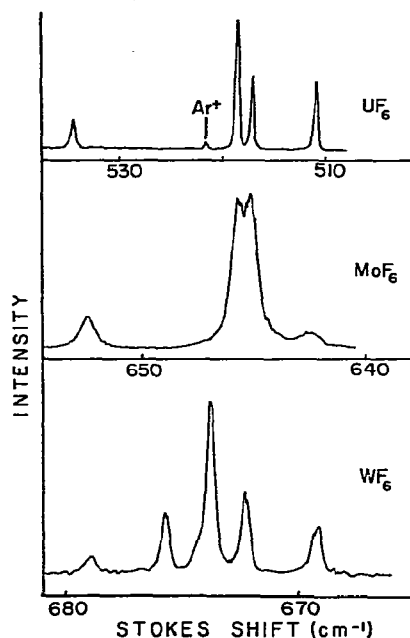


Fig. 3. High resolution Raman spectra of the ν_2 exciton region of neat MoF_6 , WF_6 and UF_6 crystals near 77 K. Notice that the scales have been shifted and normalized to point out the similarities of structure. The WF_6 spectrum is complicated due to the overlap of the ν_2 and ν_3 exciton bands (see text). The feature marked Ar^+ in the UF_6 spectrum is the 5287 Å plasma line of the laser.

ly, the crystal induced lower moments would give even larger interactions than this hexadecapole-hexadecapole term.

Fig. 3 shows the ν_2 regions of these crystals at high resolution. The four features in UF_6 and MoF_6 are seen to be quite similar when the energy scales are shifted and normalized. The four components are undoubtedly the A_g , B_{1g} , B_{2g} , and B_{3g} factor group components. The appearance of five features in the WF_6 spectrum is a consequence of the nearness of the ν_3 fundamental (711 cm^{-1} in the vapor) [3] and of the large bandwidth of that mode (see below). These circumstances create an extra peak due to overlapping bands. The identification of features deriving from solely ν_2 or ν_3 is not possible when the bands overlap. It is, however, tempting to suggest that the bands at ca. 678 cm^{-1} are associated with the ν_2 - ν_3 interaction and the features between 675 and 668 cm^{-1} are

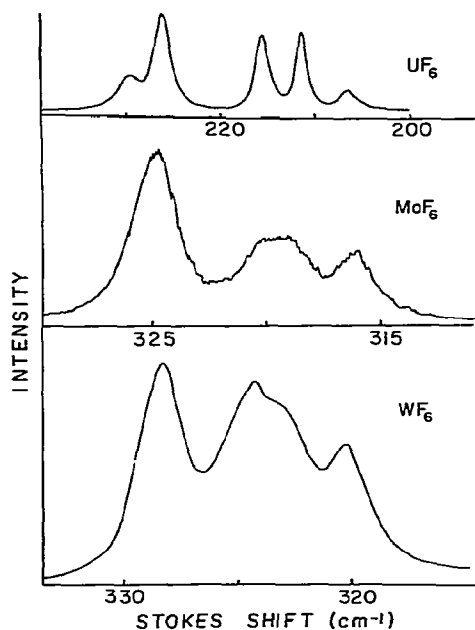


Fig. 4. High resolution Raman spectra of the ν_5 excitation region of neat MoF_6 , WF_6 , and UF_6 crystals near 77 K. The scales have been shifted and normalized to bring out the similarity of features.

mostly of ν_2 character.

In the ν_5 region (fig. 4) the UF_6 spectrum displays five of the predicted six components. The WF_6 and MoF_6 spectra suggest more than three features because of the inflections and linewidths. Again, the great similarity of these spectra is apparent when the energy scales are shifted and normalized. As for the ν_2 band, the structure in UF_6 is about twice as large as in WF_6 and MoF_6 . The greater polarizability of UF_6 with respect to the other two compounds (inferred from the ordering of the lowest charge transfer transitions of the molecules) has probably an important role in determining this. It is interesting to note that the ordering of the vibrational frequencies follows these same systematics.

The ν_3 regions are displayed in fig. 5. Recalling that ν_3 overlaps with the ν_2 band in WF_6 the similarity of the other two bands again stands out. There is interference by the intense totally symmetric transition at high energy; however, the observation of five peaks in the UF_6 spectrum nearly fulfills the factor

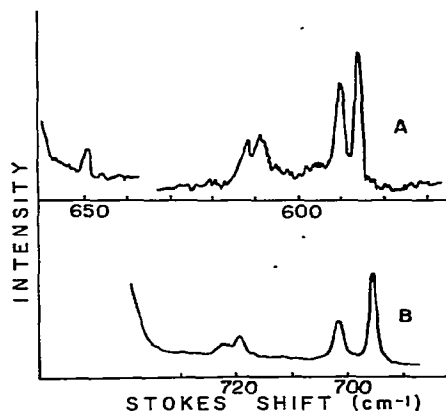


Fig. 5. High resolution Raman spectra of the ν_3 exciton region of neat crystals near 77 K. (A) is UF_6 and (B) is MoF_6 . The WF_6 spectrum has been omitted because of the absence of readily identifiable ν_3 structure due to the overlap with the ν_2 exciton band. The high energy feature (ca. 650 cm^{-1}) in UF_6 is included in the exciton band based on a comparison with the ν_3 and $\nu_1 + \nu_3$ infrared absorption spectra of ref. [9]. Similar slits and powers were used as those used to obtain the other portion of the spectrum.

group prediction. It is likely that the high energy component in MoF_6 similar to that in UF_6 is buried under the ν_1 peak. In the octahedral molecule this mode is electric dipole allowed. Again, invoking multipolar excitonic interactions it is not surprising that this band exhibits the largest spread of $k = 0$ components.

The ν_4 and ν_6 bands are most intense in UF_6 crystals (fig. 6). Their proximity to the ν_5 band suggests a crystal induced Fermi resonance mechanism is responsible for the observed enhancement with respect to MoF_6 and WF_6 transitions. UF_6 molecules are also more distorted in the solid than are MoF_6 molecules and this lower symmetry could additionally generate more intensity in the ν_4 and ν_6 transitions. However, the similar intensities in the ν_3 regions of these crystals and the greater intensity of ν_4 (closer to ν_5) over ν_6 in all crystals argues for the importance of a Fermi resonance mechanism.

Not all predicted components were observed in this region. Some may be masked by the ν_5 band and some may not be resolved since relatively wide slits were necessary to obtain measurable signals. In MoF_6 and WF_6 the ν_4 – ν_6 regions are too weak to be of much additional value over and above the previously

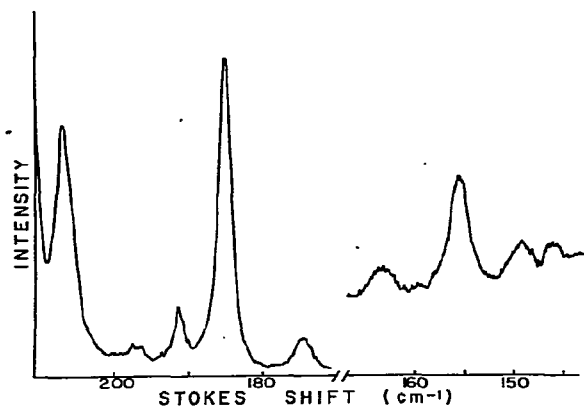


Fig. 6. Medium resolution spectra of the ν_6 (140–170 cm^{-1}) and ν_4 (180–200 cm^{-1}) exciton regions of neat UF_6 crystal near 77 K. The feature at 207 cm^{-1} has been assigned to ν_5 . $I(\nu_5) \gg I(\nu_6)$. Some of the transitions of the ν_6 band may be masked by ν_4 intensity and some of the ν_4 transitions probably lie under the ν_5 intensity.

reported two-particle ReF_6 – MF_6 vibronic transitions [11] or the $2\nu_6$ peaks discussed below.

5.2. Combinations and overtones of internal modes

Various weak features corresponding to combinations and overtones of the internal vibrational modes have been observed. Fig. 7 shows the region between the intense ν_5 and ν_2 features in the UF_6 and MoF_6 crystals. Discussion of these bands in terms of crystal states is rather involved. Besides the crystal states that could be derived from the molecular combination or overtone levels (single particle states), there are crystal states corresponding to the creation of the individual vibrations on separate molecules (two-particle states). The observation of broad bands without sharp features is an indication of two-particle character. $k=0$ selection rules can be satisfied by states created from the convolution of two bands in the latter situation. The number of such states is approximately equal to the number of molecules in the crystal. This result is quite different from the one predicted by a factor group analysis for single particle states. Expectations for this latter case would indicate relatively few sharp, well-separated features. As with all neat crystal $k=0$ structures, the center of gravity of the observed two-particle structure need not (and in gen-

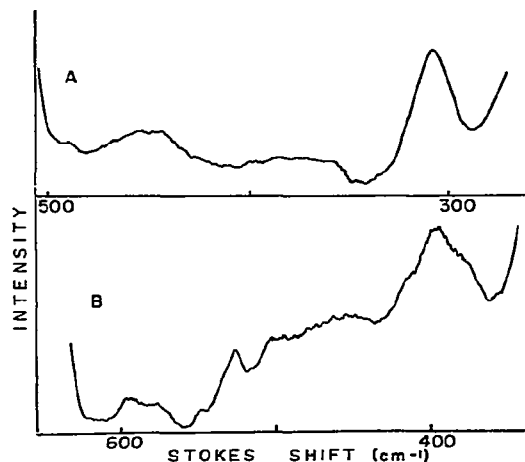


Fig. 7. Raman spectra of the bending mode combination and overtone regions in neat crystals near 77 K. A is UF_6 and B is MoF_6 . No sharp features were observed in these regions indicating a high density of Raman active $k=0$ components.

eral does not) fall at the frequency of the band center. This area will be covered in more detail in the following paper.

5.3. External modes

Fig. 8 displays the energy region below the lowest internal mode. This portion of the spectrum of neat crystal ReF_6 at 77 K has been added to aid in the assignment of the features. As discussed in section 2 and summarized in table 1, there will be twelve Raman allowed $k=0$ phonons. While formally they may be mixtures of translational and librational modes, there is some indication that the mixing is not severe. Since the phonon sideband structure observed in the $2\ \mu\text{m}$ absorption spectrum of ReF_6 doped into these crystals is quite similar to the observed $k=0$ grouping of phonons, the dispersion is probably not large, as is expected for optical phonon branches. If this is true, it is probably also true that translation–libration mixing will not be important at $k=0$, unless the same symmetry translation and libration states are close in energy.

To test this hypothesis consider the following model for the external modes based on the idea that all of these molecules “look” nearly identical from the ex-

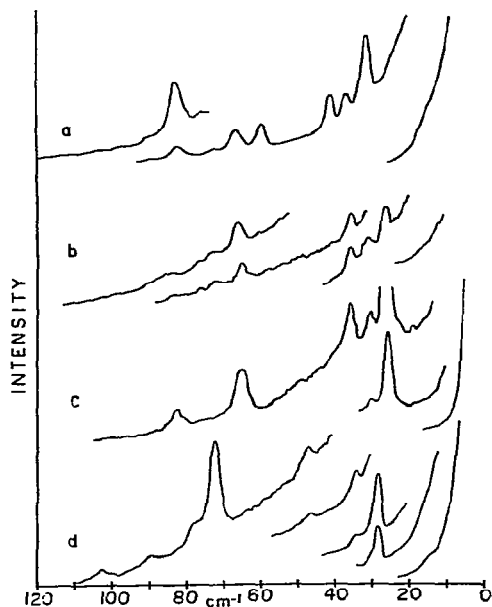


Fig. 8. Raman spectra of the phonon region of neat crystals near 77 K. The key is: (a) MoF₆; (b) WF₆; (c) ReF₆; (d) UF₆. The spectra are presented in this overlapping linear intensity manner to bring out the structure which is weak relative to the Rayleigh plus Brillouin scatter. The intense feature near 26 cm⁻¹ in ReF₆ is electronic Raman scattering to the upper levels of the split G_{3/2g} (Γ₈ fourfold degenerate) electronic ground state.

terior. Harmonic oscillator (phonon) frequencies are given by $(k/m)^{1/2}/2\pi$ in which k is the force constant and m is the reduced mass for the motion. If it is assumed that the force constants for and descriptions of each normal mode remain unchanged from crystal to crystal and that the external motions are either pure translation or pure rotation (the reduced masses are thereby proportional to the molecular weight M or the molecular moments of inertia I), then letting i index the phonon mode,

$$m_i = A_i M,$$

or

$$m_i = A_i I.$$

The observed frequencies will then be directly proportional to either $M^{-1/2}$ or $I^{-1/2}$:

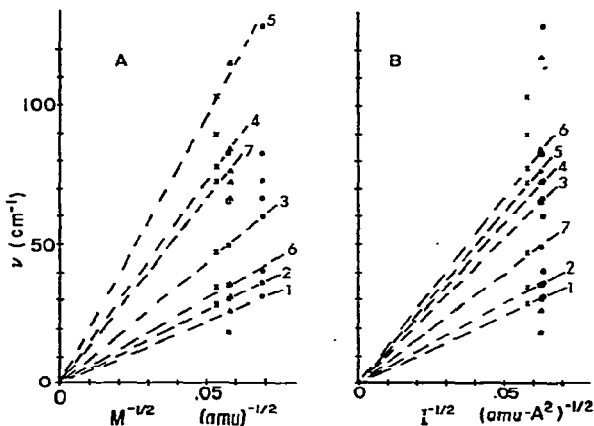


Fig. 9. Evaluation of the idealized pure translational and pure rotational phonon model discussed in the text. Plotted are the experimental frequencies ν_i ($\times = \text{UF}_6$; $\square = \text{ReF}_6$; $\triangle = \text{WF}_6$; $\circ = \text{MoF}_6$). The dashed lines are plots of eq. (1) (section 5.3) for given arbitrary values of the slope. Values for M and I are given in table 5. Lines which describe a given phonon mode are required to pass through the origin and several data points. (A) refers to purely translational motion and (B) refers to purely rotational motion. The assignments are summarized in table 6.

$$\begin{aligned} \nu_i &= [k_i/4\pi^2 A_i]^{1/2} M^{-1/2}, \\ \nu_i &= [k_i/4\pi^2 A_i]^{1/2} I^{-1/2}. \end{aligned} \quad (1)$$

Fig. 9 displays the observed frequencies plotted in this manner. Various lines indicate a particular phonon motion.

A few words should be said about the determination of moments of inertia. The recent neutron diffraction data for MoF₆ and UF₆ were examined to determine the displacement of the central metal from the center of mass of the fluoride atoms. In MoF₆ the displacement was identically zero while in UF₆ the displacement was 0.073 Å in the c direction. This value was well below the accumulated errors, so the uranium atom has been treated as if it were at the center of mass. Table 5 is a listing of the parameter used, assuming isotropic moment of inertia tensors.

It was possible with a choice of twelve phonon modes to fit all but two observed peaks. The 18.4 cm⁻¹ state in ReF₆ is probably perturbed by the low energy electronic exciton band and the isolated occurrence of the 89.8 cm⁻¹ peak in UF₆ is unexplained. Two of the phonons were not clearly identified

Table 5
Summary of molecular parameters used to evaluate phonon modes

Molecule	M-F distance (Å)			Moment of inertia (au Å ²)	Molecular weight (au)
	electron diffraction	crystal structure	adopted value		
MoF ₆	1.820	1.809	1.81	249.0	209.9
WF ₆	1.833		1.83	254.5	297.9
ReF ₆	1.832		1.83	254.5	300.2
UF ₆	1.996	1.97	1.97	294.9	352.0

as translational or librational since they fit into either graph. It would be interesting to test this assignment with polarization studies to prove the similar mode properties within each series. These data are summarized in table 6. The model can be seen, however, to be an appropriate description of the phonon modes; apparently both force constants and external mode descriptions remain unchanged throughout this series of crystals.

One might be tempted to utilize the isotope product and sum rules to help identify the phonons. But, in fact, it is exactly the generalization of the conservation of force constants and description of motions to complete irreducible representations (rather than each individual motion as done here) which forms the basis of that technique. No new information can be gained since product and sum rules are automatically satisfied for any combination of the phonon series. More

explicitly for any combination of phonons the ratio of products of frequencies between crystals is (*i* labels translational and *j* labels libration phonons),

$$\begin{aligned} & \left\{ \prod_i \frac{(\nu_i)_{\text{MF}_6}^2}{(\nu_i)_{\text{M}'\text{F}_6}^2} \right\} \left\{ \prod_j \frac{(\nu_j)_{\text{MF}_6}^2}{(\nu_j)_{\text{M}'\text{F}_6}^2} \right\} \\ &= \left\{ \prod_i \frac{k_i/A_i(M)_{\text{MF}_6}}{k_i/A_i(M)_{\text{M}'\text{F}_6}} \right\} \left\{ \prod_j \frac{k_j/A_j(I)_{\text{MF}_6}}{k_j/A_j(I)_{\text{M}'\text{F}_6}} \right\} \\ &= [(M)_{\text{M}'\text{F}_6}/(M)_{\text{MF}_6}]^{n_i} [(I)_{\text{M}'\text{F}_6}/(I)_{\text{MF}_6}]^{n_j}, \end{aligned}$$

in which there are n_i and n_j terms in the respective products. This is exactly the product rule which is required to hold for all modes belonging to one irreducible representation. Such an expression is only useful when it fails to hold for the other combinations of vibrations. These relations are valid, of course, be-

Table 6
Summary of phonon assignments based on the analysis of section 5.3. Assignments L_{*i*} and T_{*i*} are based on fig. 9 and are indicated on the specific mode lines

MoF ₆		WF ₆		ReF ₆		UF ₆	
energy (cm ⁻¹)	assignment	energy (cm ⁻¹)	assignment	energy (cm ⁻¹)	assignment	energy (cm ⁻¹)	assignment
30.9	L ₁ , T ₁	26.0	T ₁	18.4		28.4	L ₁ , T ₂
36.4	L ₂ , T ₂	30.7	L ₁ , T ₂	25.6 a)	(T ₁)	34.6	L ₂ , T ₆
40.7	T ₆	35.5	L ₂ , T ₆	29.9	L ₁ , T ₂	47.0	L ₇ = T ₃
59.6	T ₃	65.5	L ₃	35.4	L ₂ , T ₆	72.5	L ₅ = T ₇
66.6	L ₃	72.4	L ₄	49.2	L ₇ = T ₃ b)	77.8	L ₆ , T ₄
72.7	L ₄	76.5	L ₅ = T ₇ b)	65.4	L ₃	89.8	
82.7	L ₆	84.4	L ₆ , T ₄	82.9	L ₆ , T ₄	103.2	T ₅
128	T ₅	115	T ₅				

a) This peak also corresponds to a Raman transition to a low lying electronic state.

b) This phonon could be either a translational or librational motion based on fig. 9.

cause of the highly restrictive nature of eqs. (1).

4. Summary

Raman spectra of neat crystals of MoF_6 , WF_6 and UF_6 have been obtained and discussed in terms of the internal and external modes of the molecules. The spectra of the fundamental regions are consistent with factor group predictions based on the published crystal structures. Molecular and crystal Fermi resonances are important in understanding differences between the various crystal spectra and for explaining intensity distributions. The excitonic structures are remarkably alike when energy scales are normalized for each fundamental region. The similarity is a crystal phenomena and the energy scaling is attributed to differences in molecular properties (e.g., polarizability and electric dipole derivatives). The external modes have been fit to a model treating the optical phonons as crystal independent pure translational and librational normal modes.

References

- [1] G.L. Goodman and B. Weinstock, *Advan. Chem. Phys.* 9 (1965) 169.
- [2] J.P. Aldridge, H. Filip, H. Flicker, R.F. Holland, R.S. McDowell, N.G. Nereson and K. Fox, *J. Mol. Spectry.* 58 (1975) 165.
- [3] H.H. Claassen, G.L. Goodman, J.H. Holloway and H. Selig, *J. Chem. Phys.* 53 (1970) 341.
- [4] R.S. McDowell, R.J. Sherman, L.B. Asprey and R.C. Kennedy, *J. Chem. Phys.* 62 (1975) 3974.
- [5] R.S. McDowell and L.B. Asprey, *J. Mol. Spectry.* 48 (1973) 254.
- [6] R.S. McDowell, L.B. Asprey and R.T. Paine, *J. Chem. Phys.* 61 (1974) 3571.
- [7] K. Fox, B.J. Krohn and W.H. Shaffer, Paper RM11, Thirty-First Symposium on Molecular Spectroscopy (Ohio State University, Columbus, Ohio, June 14-18, 1976).
- [8] K.H. Hellberg, A. Muller and O. Glemesen, *Z. Naturforsch.* 21b (1966) 118.
- [9] R. Bougon and P. Rigny, *C.R. Acad. Sci. Paris C263* (1966) 1321.
- [10] M. Gilbert and M. Drifford, in: *Advances in Raman spectroscopy*, ed. J.P. Mathieu (Heydon and Sons, New York, 1973) p. 204.
- [11] E.R. Bernstein and G.R. Meredith, *J. Chem. Phys.* 64 (1976) 375.
- [12] J.D. Webb, unpublished results.
- [13] R.S. McDowell, Los Alamos Scientific Laboratory Internal Document CNC-3-75: 18 (May 1, 1975).
- [14] R. Kopelman, *Excited states*, Vol. 2, ed. E.C. Lim (Academic Press, 1975) p. 34.